Pyrolysis and Ignition of a Polymer by Transient Irradiation

Izabella Vermesi[a], Nils Roenner[a], Paolo Pironi[b], Rory Hadden[b], Guillermo Rein[a,*]

[a] *Imperial College London, Department of Mechanical Engineering, London SW7 2AZ, United Kingdom*
[b] *BRE Centre for Fire Safety Engineering, University of Edinburgh, Edinburgh EH9 3JL, United Kingdom*

Abstract

Pyrolysis is the thermochemical process that leads to the ignition of a solid fuel and a key mechanism in flame spread and fire growth. Because polymer materials are flammable and ubiquitous in the modern environment, the understanding of polymer pyrolysis is thus essential to tackle accidental fires. In this paper, we used transient irradiation as an external source of heat to study the process of pyrolysis and ignition of a polymer sample. While previous ignition studies use constant irradiation, transient irradiation is the most frequent condition found in accidental fires, but it lacks a theoretical framework since it has been largely ignored in the literature. Moreover, transient irradiation is a more comprehensive case for the understanding of pyrolysis where nonlinear heat transfer effects challenge the validity of solid-phase criteria for flaming ignition developed previously. We propose here that transient irradiation is the general problem to solid fuel ignition of which constant irradiation is a particular solution. In order to investigate how this novel heat source influences polymer pyrolysis and flammability, numerical simulations and experiments have been conducted on Poly(methyl methacrylate) (PMMA) samples 100mm by 100mm and 30mm deep exposed to a range of parabolic pulses of irradiation. The 1D model, coded in GPyro, uses heat and mass transfer and single-step heterogeneous chemistry, with temperature dependent properties. The predictions are compared to experiments conducted in the Fire Propagation Apparatus using both constant and transient irradiation conditions. The experiments validate the temperature predictions of the model and also provide the time to ignition. The model then complements the experiments by calculating the mass loss rate. A series of 16 parabolic pulses (including repeats) are investigated with a range of peak irradiation from 25 to 45 kW/m^2, while the time to peak ranges from 280 to 480s. For these pulses, the time to ignition measurements range from 300 to 483s. The model can predict the in-depth temperature profiles with an average error lower than 9%. Model and experiments are then combined to study the validity of the solid-phase criteria for flaming ignition found in the literature, namely critical temperature, critical mass loss rate, critical energy and critical time-energy squared. We find that of these criteria, the best predictions are provided by the critical mass loss rate followed by the critical temperature, and the worst is the critical energy. Further analysis reveals the novel concept of simultaneous threshold values. While the mass loss rate is below 3g/m^2 and the surface temperature is below 305°C, ignition does not occur. Therefore these threshold values when exceeded simultaneously establish the earliest time possible for ignition.

Keywords: pyrolysis, radiation, heat transfer, polymethyl methacrylate

Nomenclature

Symbol	Description
A	pre-exponential factor
C	proportionality factor between time and energy-squared
c_p	heat capacity
E	activation energy
ΔH	heat of reaction
h_c	convective heat transfer coefficient
k	thermal conductivity
L	depth of the the sample
$\dot{m}''$	mass flux per unit area
m''	mass per unit area
Q	energy
$\dot{q}''$	heat flux
$\dot{Q}'''$	heat generation per unit volume
R	universal gas constant
T	temperature
t	time
Y	mass fraction
z	depth into the sample

Greek Letters

Symbol	Description
ε	emissivity
κ	radiative absorption coefficient
$\dot{\omega}'''$	reaction rate per unit volume
ρ	density
σ	Stefan-Boltzmann constant

Subscripts

Symbol	Description

*Corresponding author
Email address: g.rein@imperial.ac.uk (Guillermo Rein)
[1]Phone Number: +44 (0)20 7594 7036

0	initial
Al	aluminium
e	external
d	destruction
g	gas
i	condensed-phase species index
ig	at ignition
p	at peak
r	in-depth radiation
s	solid

1. Introduction

Fire is a complex phenomenon that encompasses a series of chemical and physical processes [1]. Before the combustible material can undergo combustion and release heat, it has to undergo ignition, which is a critical process that determines the initial growth of the fire [2]. Ignition is the onset of combustion, and flame ignition the process by which the fast, exothermic, homogenous reaction is started, which then spreads further in the material, causing mass burning [3].

However, before flaming ignition can occur, the solid fuel has to become gaseous [2], [3], [4]. The process through which the solid undergoes a chemical decomposition and transforms into a gaseous fuel is called pyrolysis [3], [4]. Because the molecules of solid hydrocarbon fuels like synthetic polymers or wood are large, they cannot be oxidized directly. Therefore, when exposed to heat, these molecules irreversibly decompose into smaller hydrocarbon chains which emerge as gas [5]. Under the right conditions, these can ignite above the surface of the solid. Pyrolysis is the key process in the burning of solid fuels, because the rate at which a material transforms into a gas phase fuel governs the timing of ignition and the energy release rate in the subsequent flames [4].

Most ignition studies consider constant irradiation representing the radiant irradiation from the heat source [3]. The exception to the ignition studies is the work by Reszka et al. [6] which considers a linearly increasing irradiation on a series of fuel types, and the work by Belcher et al. [7] which uses parabolic heat pulses. While using a constant irradiation is convenient due to its simplicity, this scenario is not realistic. Moreover, transient irradiation is a more comprehensive case for the understanding of pyrolysis where nonlinear heat transfer effects challenge the validity of solid-phase criteria for flaming ignition developed previously. We propose here that transient irradiation is the general problem to solid fuel ignition of which constant irradiation is a particular solution. It is essential to understand how and when ignition is reached with both constant and transient irradiation. This paper aims to carry out that study by combining numerical and experimental work. A parabolic pulse is chosen here because it is the simplest curve including both growth and decay.

The investigation of the ignition is done by comparing complementary experimental and computational works that use transient irradiation to investigate the pyrolysis of Poly(methyl methacrylate)(PMMA), a polymer widely studied in fire science. The experiments measured the temperatures of the PMMA samples heated by irradiation pulse, thus providing validation for the numerical model.

This paper begins by summarizing the theoretical background on the classical ignition theory and four different ignition criteria found in the literature: critical energy, critical temperature, critical mass flux and time-energy squared. Afterwards, the experimental work is presented. The computational work, performed in a 1D pyrolysis model, GPyro [8], is then presented and validated using benchmark experiments by Kashiwagi et al. [9]. The results of the simulations are then compared to the transient irradiation experiments. Finally, the ignition criteria are assessed with respect to both constant and transient irradiation.

2. Classical Ignition

Pyrolysis occurs inside the solid phase, and produces the gases necessary to feed the flame. In order to study flame ignition with a focus on solid-phase phenomena, there is need to replace the gas phase and invoke an ignition criterion. This criterion describes when ignition of the gas phase would take place by referring to conditions in the solid phase alone. In the literature, there are four criteria for piloted ignition. All four are empirical but based on combustion theories of different degree of development. These are the critical energy, critical temperature, critical mass flux and time-energy squared.

For a thermally thick solid, the critical temperature criterion leads to Eq. 1 to establish the time to ignition calculated from the assumption of a critical surface temperature and a constant irradiation [4]. It is the most commonly used ignition criterion. It takes into account two main parameters, namely the ignition temperature and the thermal inertia of the fuel. However, this approach has several limitations. The greatest limitation is the difficulty of measuring the critical temperature [5], and its variation with regards to external heat flux and environmental conditions such as oxygen concentration. Therefore, the critical temperature criterion cannot give a certain value applicable for each fuel, but it varies with conditions under which it was determined [4], [10].

$$\frac{1}{\sqrt{t_{ig}}} = \frac{2}{\sqrt{\pi}\sqrt{k\rho c}} \frac{\dot{q}''_e}{T_{ig} - T_0} \tag{1}$$

The critical mass loss rate is considered the most fundamental criterion. It assumes that ignition takes place when a critical flow of pyrolyzate mixes with air such that the mixture surpasses the lower flammability limit at the location of the pilot [3]. However, the experimental measurements are quite difficult, because the mass loss rate before ignition is very low [5]. Rich et al. [11] have proposed a theoretical model that relates the critical mass flux

necessary for ignition to fuel properties using Spalding's number [12] and to environmental characteristics [11].

The critical energy criterion states that a sample will ignite after absorbing a certain amount of energy. The energy criterion relies on a series of simplifications, such as lack of heat losses and a constant ignition temperature [5]. Therefore, the criterion provides ranges of critical energy rather than a single value for each material.

$$Q_{ig} = \int_0^{t_{ig}} \dot{q}''_e dt \tag{2}$$

The only criterion in the literature developed for transient irradiation is the time-energy squared correlation. This has been developed by Reszka et al.[6] and calculates the time to ignition by finding the squared integral of the incident irradiation up to the elapsed time. This method is applicable for incident irradiation fluxes that grow linearly. The methodology for this criterion relies on the linear dependency between $t_{ig}^{-1/2}$ and $\dot{q}"_{ext}$ and results in Eq. 3, where C represents the linearity coefficient and it depends on the irradiation scenario, having different values for constant irradiation, for linear irradiation and for parabolic pulses.

$$Q_{ig}^2/t_{ig} = C \tag{3}$$

The four ignition criteria are applied to PMMA with values taken from the literature. PMMA, commonly called plexiglass, is one of the most common polymers studied in fire science, therefore there is substantial experimental and computational data available for comparison. It is a non-charring thermoplastic polymer that has different grades and blends. A commercial cast grade PMMA is used for the experiments in this study. The ranges found in the literature for the critical parameters are presented in Table 4.

Table 4: Typical ignition criteria values for PMMA found in literature

Ignition Criteria	**Value of parameter**
Critical Energy	2 MJ/m^2 (irradiance of 30kW/m^2) [5]
Critical Mass Flux	2.0 g/m^2-s [13], 1.9-3.2 g/m^2-s [14]
Critical Temperature	250-400°C [15], 380°C [4]
Critical Time-Energy Squared	226 GJ^2/m^4-s [6]

3. Experiments

Experiments were conducted in a Fire Propagation Apparatus (FPA) using a set-up based on the standard piloted ignition test described in ASTM E2058 [16]. A specimen of the sample material was subjected to irradiation on its upper surface from an external radiant source

and a pilot flame. The irradiation was provided by four infrared heaters each containing six tungsten filament tubular quartz lamps. Parabolic irradiation-time pulses with different duration and maximum irradiation were used for each group of experiments, as shown in Table 5 and Figure 2. In-depth temperature profile was measured with four type-K thermocouples inserted parallel to the heated surface at depths of 2, 5, 8 and 10mm, as illustrated in Figure 1. The thermocouples were sheathed, thus having no exposed beads, and had a diameter of 1.5mm, which is uniform along the length of the thermocouples. This methodology has been used previously in [17] and [18] and yielded good results, with a maximum error of 10%. Because the transient heating of the material is slow, issues related to thermocouple diameter, such as lag, are negligible. In order to characterize better the heat transfer in the sample, the set-up incorporated a large aluminium block at the bottom face of the sample. Its temperature was measured by a thermocouples inserted in the centre of the block [18].

Table 5: List of experiments using parabolic irradiation pulses

Experiment no.	**Peak irradiation** (kW/m^2)	**Time to peak** (s)	**Irradiation pulse duration** (s)
1, 2, 3	30	320	640
4, 5, 6	45	320	640
7, 8, 9	25	320	640
10, 11, 12, 13	30	480	960
14, 15, 16	30	260	520

Commercial sheets of PMMA were pre-cut into 100 x 100 x 30mm samples. Prior to testing, the base of the sample and its sides were wrapped in a layer of aluminium foil. The sample and aluminium block were then tightly wrapped in a layer of ceramic paper for thermal insulation, secured by 3 pieces of thin wire wrapped around the outside. The irradiation-time pulses were generated by sampling the target parabolic curves at 10s intervals and varying the voltage applied to the lamps according to calibration. The pilot flame was ignited prior to the beginning of the test and maintained on throughout the experiment, as shown in Figure 1.

An example of temperature histories for the 30 kW/m^2 experiments with in-depth temperature measurements are presented in Figure 3. The parabolic irradiation is represented in Figure 2. The repeatability of the time-temperature pulses and the ignition delay time is very high. The sample did not ignite when subjected to a shorter pulse duration (520s) peaking at $30kW/m^2$, or to a lower peak ($25kW/m^2$).

Mass loss measurements in transient irradiation are challenging due to excessive noise and a small signal. But mass loss rate is important to understand ignition, so this paper predicts

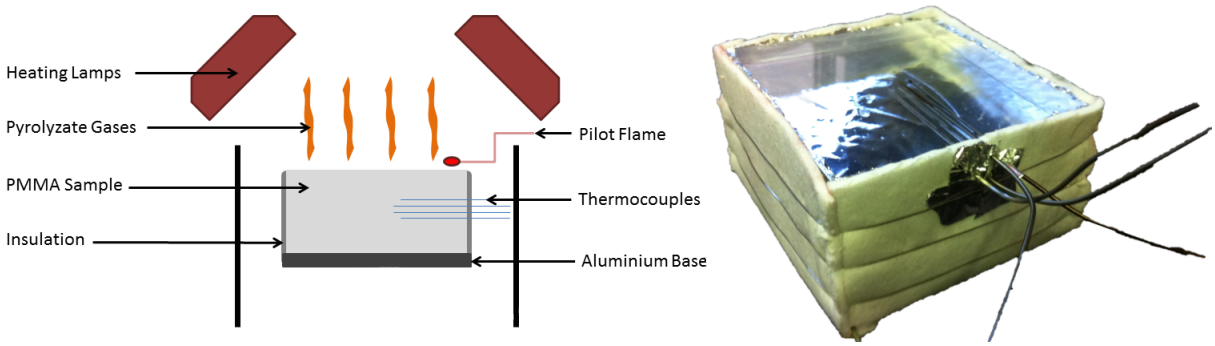

Figure 1: Sketch of the test setup (left) and a prepared PMMA sample (right)

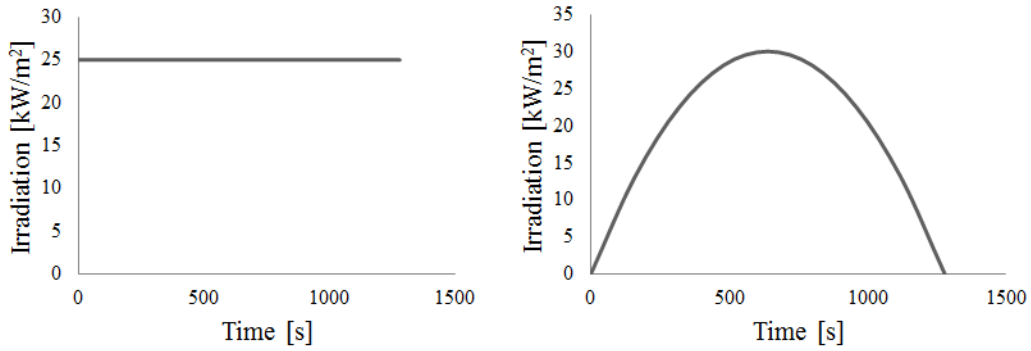

Figure 2: Constant irradiation (left), which is used in most literature and the parabolic irradiation pulse (right), applied in this paper

it numerically instead of measuring it.

To investigate a wider applicability of the results beyond the transient irradiation with the tungsten lamps of the FPA, additional data is collected under constant irradiation in a cone heater. For these tests, the samples, prepared in an identical manner as described, are placed in a calibrated cone heater under 15kW/m^2 and 20kW/m^2 irradiation.

4. Numerical Model

4.1. Gpyro

The one-dimensional (1D) numerical model for this study was done in GPyro, an open-source software that represents the state of the art in pyrolysis modelling [8]. The 1D assumption is valid for this case because the characteristic length is much larger than the thickness of the sample. The governing equations for the solid (condensed) phase are detailed in Eq. 4 for the mass, Eq. 5 for the species, and Eq. 6 for the energy. For more details, refer to [19].

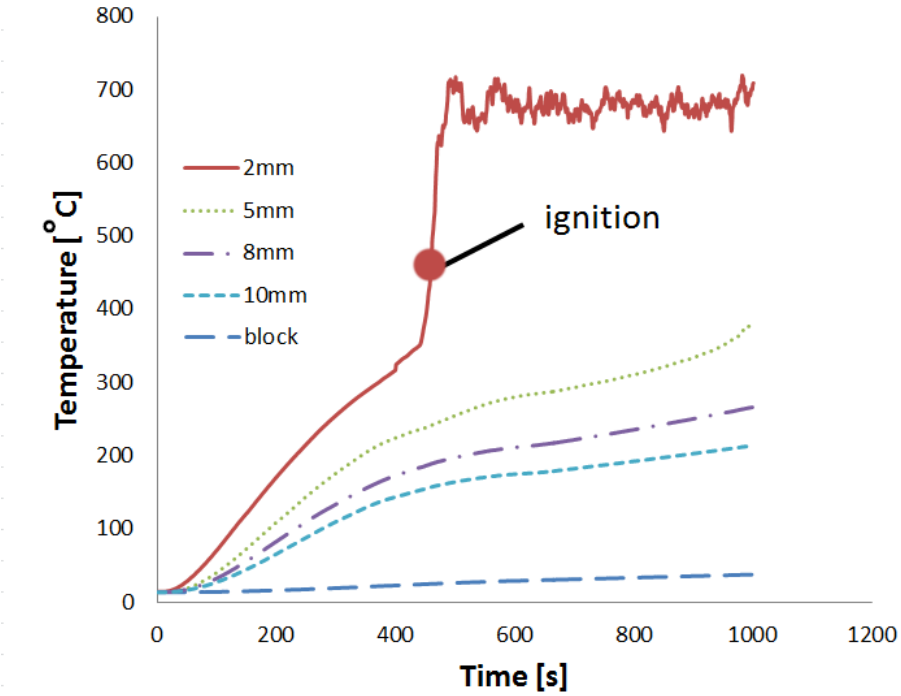

Figure 3: Average temperature-time curves for experiment 1-2: transient irradiation peaking at 30kW/m^2 after 320s

$$\frac{\partial \bar{\rho}}{\partial t} = -\dot{\omega}_g''' \tag{4}$$

$$\frac{\partial (\bar{\rho} Y_i)}{\partial t} = -\dot{\omega}_{di}''' \tag{5}$$

$$\frac{\partial (\bar{\rho}\bar{h})}{\partial t} = \frac{\partial}{\partial z}\left(\bar{k}\frac{\partial T}{\partial z}\right) + \sum_{i=1}^{K} \dot{Q}_{s,k}''' + (-\dot{\omega}_{di}''')\Delta H_s - \frac{\partial \dot{q}_r''}{\partial z} \tag{6}$$

The state of the art chemistry for PMMA pyrolysis is a three step process [10]. However, Bal and Rein [20] have shown that the heat transfer in the solid phase is dominant and the chemistry is of secondary importance in defining the pyrolysis. Therefore, a one-step reaction scheme is used as the uncertainty associated with a more complex kinetic scheme outweighs the improvements in accuracy (as confirmed in later sections).

The rate at which a material pyrolyses is described by a simple Arrhenius-type function of the temperature, presented in Eq. 7.

$$\dot{\omega}_i = \frac{\partial m_i''}{\partial t} = m_{i0}'' A_i e^{-E_i/RT} \left(\frac{m_i''}{m_{i0}''}\right)^{n_i} \tag{7}$$

The domain used in the simulations represents the experimental set-up, as shown in Figure 4. The equation for the bottom boundary (adiabatic) is shown in Eq. 8, where z=L. The sample is a two-layer system and zero contact thermal resistance is assumed between the PMMA and the aluminium. The generalized boundary condition including emissive, convective and irradiative terms, is shown in Eq. 9 and is applied at the top surface, where z=0. The in-depth absorptivity is accounted for using Eq. 10 [8]. While in-depth absorption of external radiation is important in a translucent fuel in fire conditions [10],[23] in-depth emission is not because the range of values of in-depth temperature immediately away from the free surface are low. Therefore, the in-depth emission across a PMMA sample can be accurately modelled by a surface emission of 0.95 [10].

$$-\bar{k}\frac{\partial T(L)}{\partial z} = 0 \tag{8}$$

$$-\bar{k}\frac{\partial T(0)}{\partial z} = \bar{\varepsilon}\dot{q}_e^{"} - h_c(T_s - T_0) - \bar{\varepsilon}\sigma(T^4 - T_0^4) \tag{9}$$

$$-\frac{\partial \dot{q}_r^{"}}{\partial z} = \bar{\varepsilon}\dot{q}_e^{"}\bar{\kappa}e^{-\bar{\kappa}z} \tag{10}$$

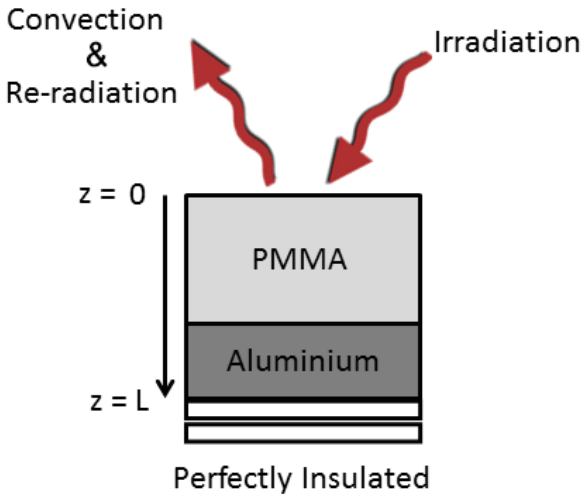

Figure 4: The computational domain and the boundary conditions

As with any numerical model, it is important to see how much the results are influenced by the discretization parameters, namely grid size and time step. The sensitivity analysis is performed using a simulation with 25kW/m^2 which peaks at 320s. The results are shown in Figure 5. Keeping a balance between accuracy and simulation time, the final values of the domain parameters are chosen: a size of 0.05mm and a time step of 0.05s.

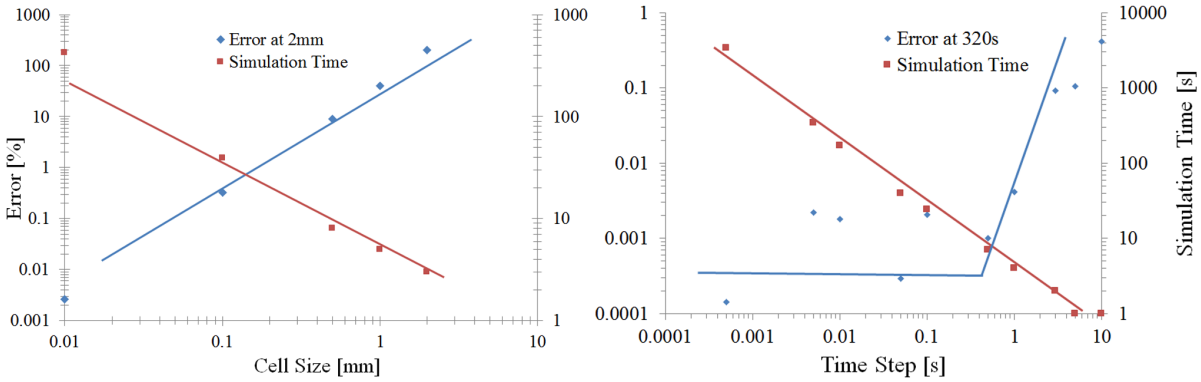

Figure 5: Error sensitivity with respect to grid size (left) and time step (right)

4.2. Model Validation Against Benchmark

To verify the simplifications adopted, the work of Kashiwagi et. al. [9] is taken as reference. The experiments were pioneering in this field and the results represent high fidelity data. Constant irradiation of a PMMA sample was studied under varying atmospheric conditions, with the temperature at surface and the mass loss measured. The experiments were conducted for 40kW/m^2 and 17kW/m^2 fluxes.

These experiments were simulated in [21] with the complexity of three step chemistry. Using this basis, the effects of the simplifications can be studied in detail and compared to well established data.

As a first step the original Lautenberger model is replicated and then the simplifications of the reduced 1-step chemistry applied. The comparison for the 40kW/m^2 experiment [9] is shown in Figure 6 . It can be seen that despite the reduction in complexity most of the accuracy of the simulation is retained. However, because these experiments are the only mass loss rate measurements that can be used for comparison with the model, it is important to note that there is a maximum error of 25% induced by the modelling assumptions. This is considered acceptable for the simulation purposes and the progression to the single-step chemistry model is made.

4.3. Parametric Study

Due to the transient nature of the scenario, most properties are considered temperature depeneant (as opposed as to the common assumption of constant effective properties, see [10] for details). Our justification is two-fold. First, there are large difference in property values of PMMA across the temperature range observed in the experiments (from 30 to 700 C approximately). Moreover, in transient irradiation, there is first heating and then cooling regimes, which is the concept of a constant effective value. This alternation is not present in constant irradiation conditions. These properties are assessed using Eq. 11, shown here

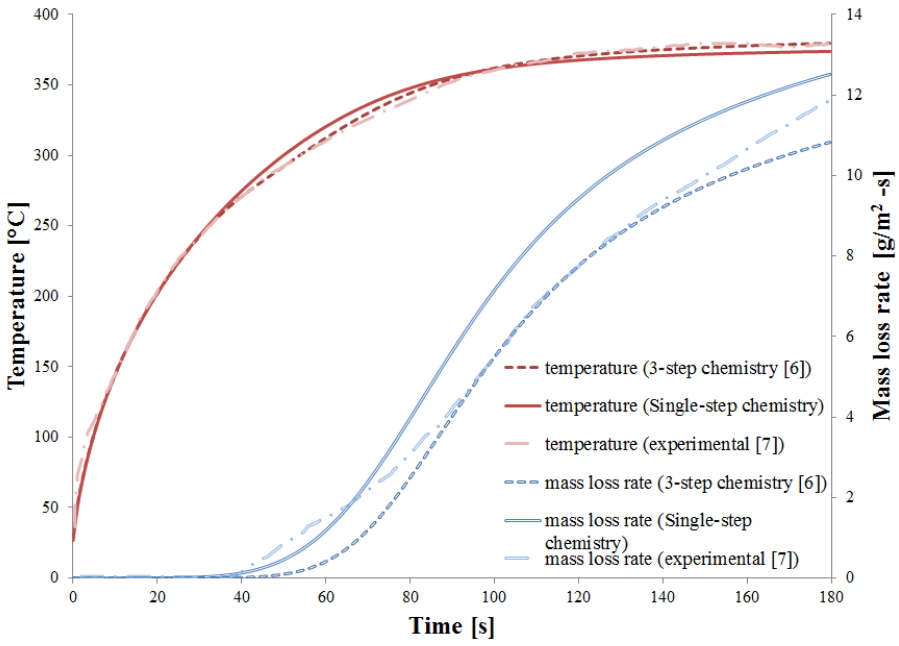

Figure 6: Validation of single-step chemistry model against Lautenberger's three-step chemistry [8]and Kashiwagi's experimental results [9]: surface temperature results for a sample exposed to heat flux of 40kW/m^2 on the left and mass loss rate results on the right

for thermal conductivity. The reference temperature T_{ref} is taken as 300K.

$$k(t) = k_0 \left(\frac{T}{T_{ref}} \right)^{n_k} \tag{11}$$

Because the material properties of PMMA as reported in the literature vary significantly, a parameter sensitivity analysis was performed to see how the temperature and mass loss respond to the change in parameters. Typical ranges for PMMA are extracted from the review by Bal [15] and the maxima and minima are compared to a base case in terms of temperature response near the surface (2mm)and in-depth (10mm), as well as the mass loss response. The analysis is presented in Figures 7 and 8. These figures show the most important material properties of the PMMA in order to obtain reliable results. Some parameters, like emissivity, influence the results mostly at the surface, whereas others, such as the in-depth absorption, are influential in-depth.

Specific heat capacity is the parameter inducing the largest variation, both at surface level and in-depth. The one that induces the least variation is the compensation effect of kinetics, which couples the parameters of pre-exponential factors and activation energy.

The model parameters for the base case are listed in Table 6 for the temperature dependent properties, Table 7 for the in-depth absorptivity, Table 8 for the properties of the aluminium block, Table 9 for the kinetics constants and Table 10 for other important parameters. To justify the chosen values for emissivity and in-depth absorptivity, in Bal et al. [10] it is shown that =1 and our equations for the in-depth absorption can reproduce in detail and with a very low error the in-depth temperature profile of PMMA for a wide range of constant irradiation levels.

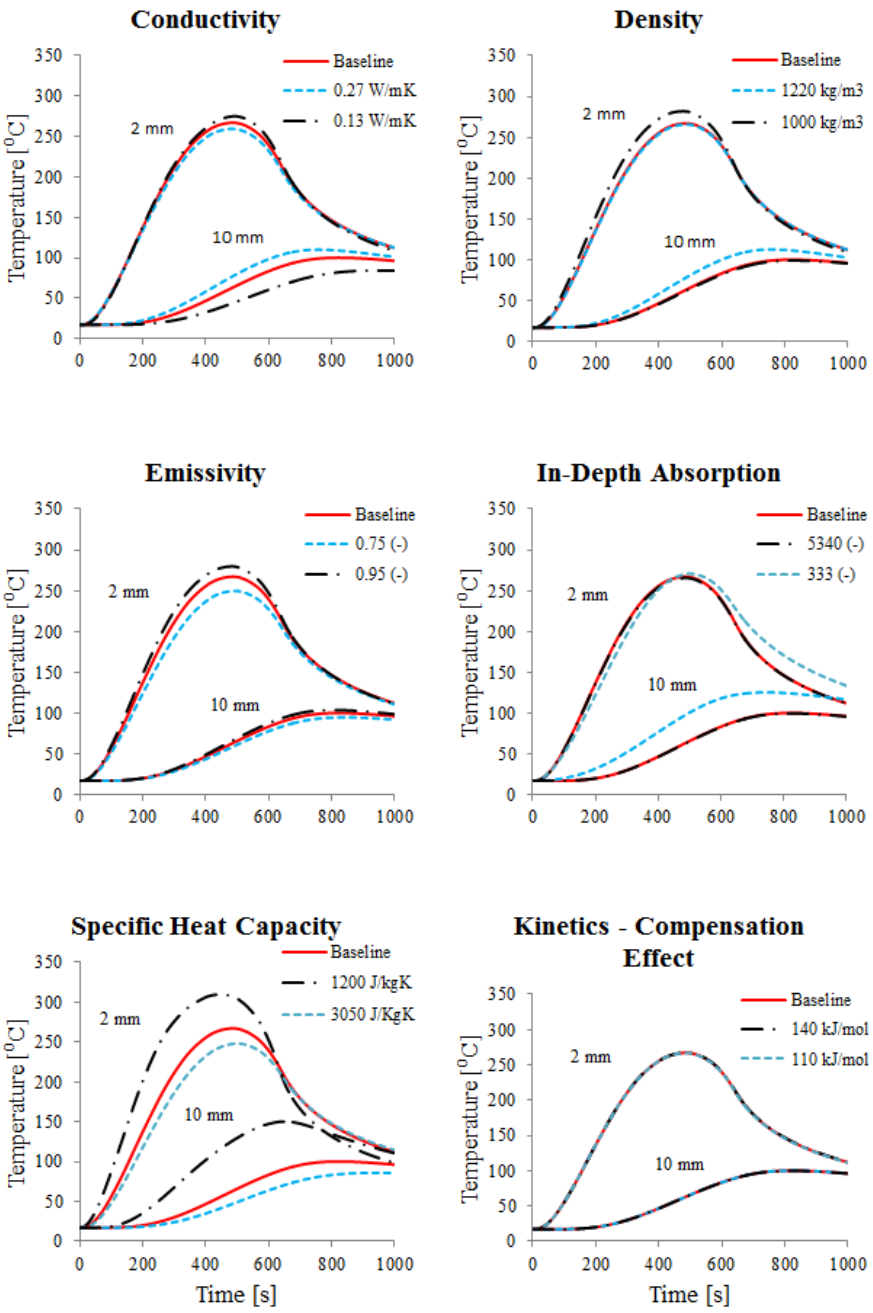

Figure 7: Sensitivity of the predicted surface temperatures to varying material properties. Predictions at two depths into the sample are reported: 2 mm and 10 mm from the surface.

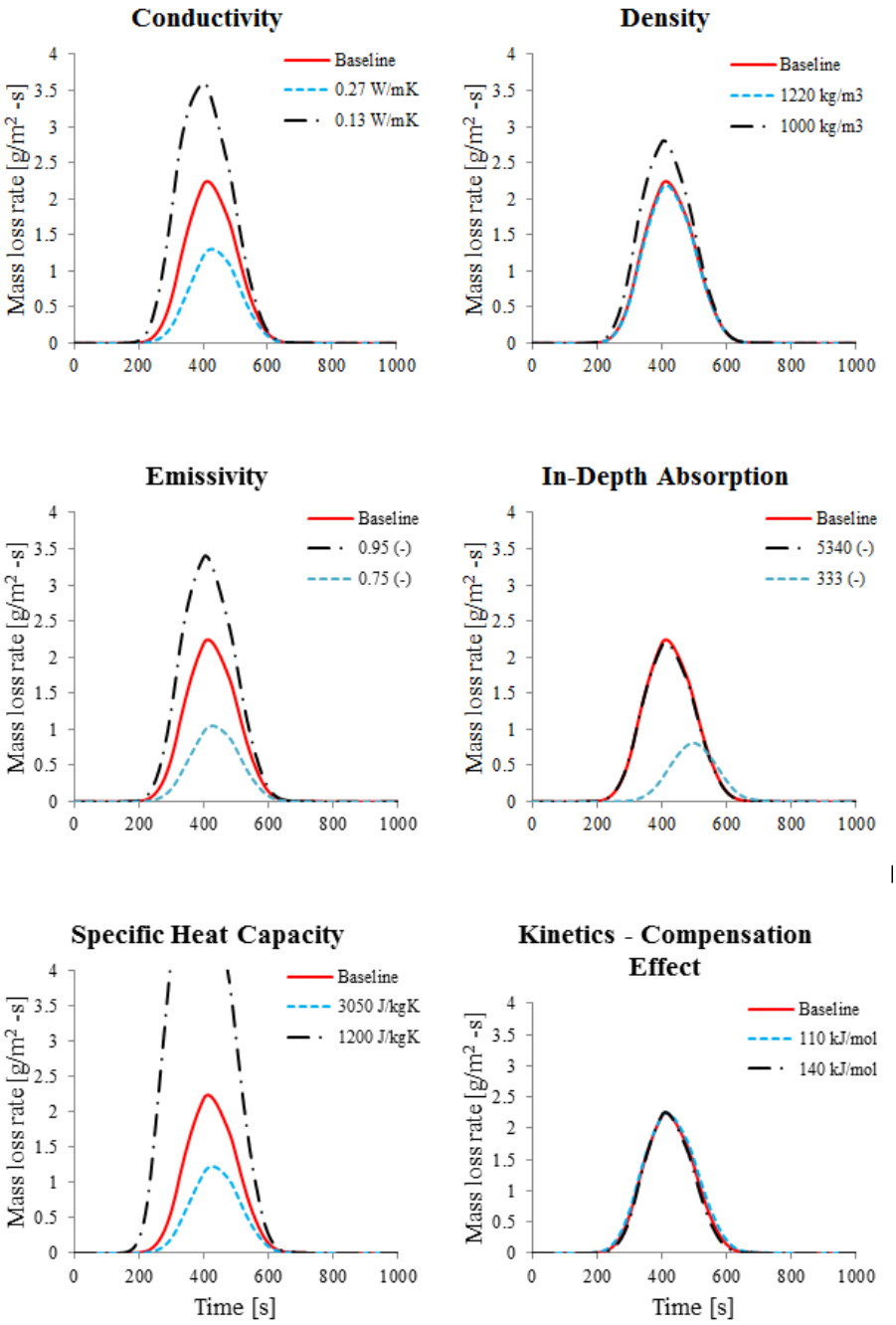

Figure 8: Sensitivity of the predicted mass loss rate to varying material properties.

Table 6: Baseline modelling parameters: temperature dependent properties for PMMA [21]

Temperature dependent parameters			
Property	*Value*	*Exponent Value*	*Units*
Thermal Conductivity k	0.2	-0.19	W/mK
Density ρ	1190	-0.12	kg/m^3
Specific Heat Capacity c_p	1606	0.89	J/kgK

Table 7: Baseline modelling parameters: in-depth absorptivity κ [23]

In depth absorptivity κ		
Heat Source	*Value*	*Units*
Tungsten Lamp	225	m^{-1}
Cone	1000	m^{-1}

Table 8: Baseline modelling parameters: properties of aluminium block [22]

Properties of aluminium		
Property	*Value*	*Units*
Thermal Conductivity k_{Al}	244	W/mK
Density ρ_{Al}	2700	kg/m^3
Specific Heat Capacity $c_{p,Al}$	921	J/kgK
Emissivity of Aluminium ϵ	1	-

Table 9: Baseline values for kinetic constants [9]

Kinetic constants		
Property	*Value*	*Units*
Pre-exponential Factor A	200	s^{-1}x10^6
Activation Energy E	125	kJ/mol
Heat of Reaction ΔH_s	540	kJ/kg
Reaction Order n	1	-

Table 10: Miscellaneous properties

Miscellaneous properties		
Property	*Value*	*Units*
Convective Heat Transfer Coefficient at Top Surface h_c	10	W/m^2K
Gas Phase Specific Heat Capacity c_p	1003	kJ/kgK
Ambient Temperature T (adjusted for each experiment)	20	°C
Surface emissivity of PMMA ϵ [10]	0.95	

5. Transient Irradiation Results

The first experiments studied numerically are those of constant irradiation, because it is the most common test condition in the literature and the simplest irradiation condition. Therefore, obtaining good results in a constant irradiation case is a prerequisite to model more comprehensive conditions. The two cases presented in Figures 9 and 10 replicate the two constant irradiation test case done in the complementary experiments. The simulations run up to 520s, when ignition was observed in the case of the $20kW/m^2$ irradiation and when the thermocouples became exposed due to the sample mass lost in the $15kW/m^2$ case, which did not ignite. The experiments were done only once. The temperature results show excellent agreement, with an average error of 3.2%.

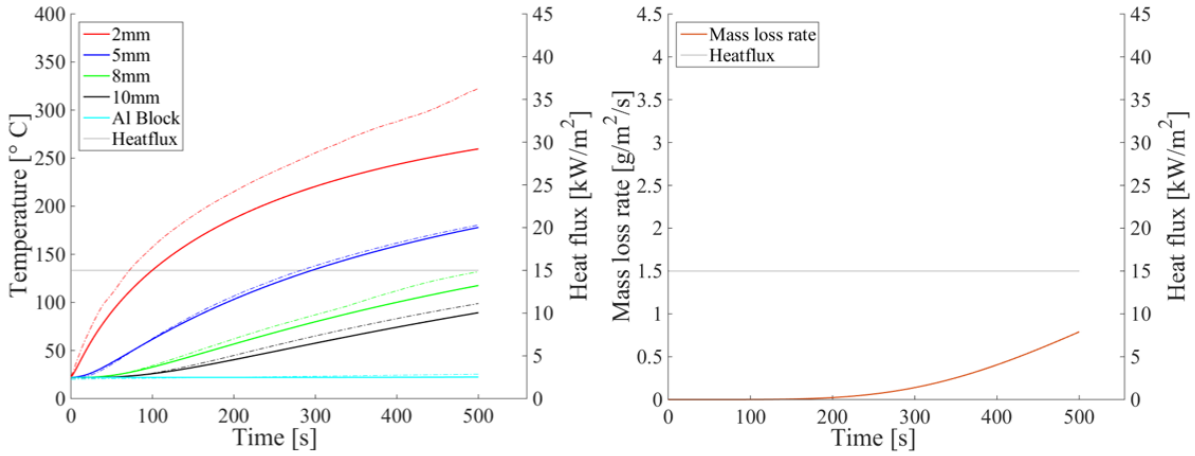

Figure 9: Constant irradiation of $15kW/m^2$: Temperature(a) and predicted mass loss rate (b) at different depths of a PMMA sample; Predictions shown in solid, experiments with dashed line (Experiments conducted in cone calorimeter)

For the transient irradiation, all the experiments are predicted numerically in Figures 11 to 15. The temperature and mass loss response are shown in comparison with the experimental results. They capture the peak irradiation, as well as the time to peak, marking the first

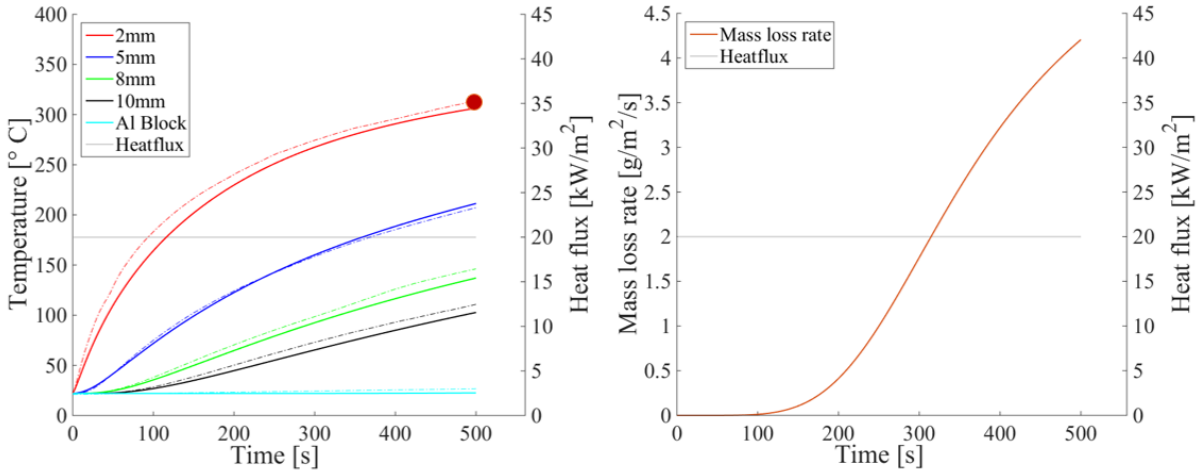

Figure 10: Constant irradiation of 20kW/m^2: Temperature(a) and predicted mass loss rate (b) at different depths of a PMMA sample; Predictions shown in solid, experiments with dashed line (Experiments conducted in cone calorimeter)

time that a transient irradiation model is used to predict the pyrolysis of PMMA. The errors are in the range of 10% for all the cases, with a large contribution to this error being brought by the deviations at the aluminium block. By predicting the mass loss rate, this model also complements the experimental work, which allows for the evaluation of the critical mass loss rate criterion.

The ignition results and the irradiation pulses are summarized in Figure 16. The cases that did not ignite, namely the reduced time to peak and the reduced peak irradiation, are in dashed line and the entire irradiation pulse is shown. In the remaining cases, the ones where ignition occurred, the irradiation pulse is shown until the ignition time.

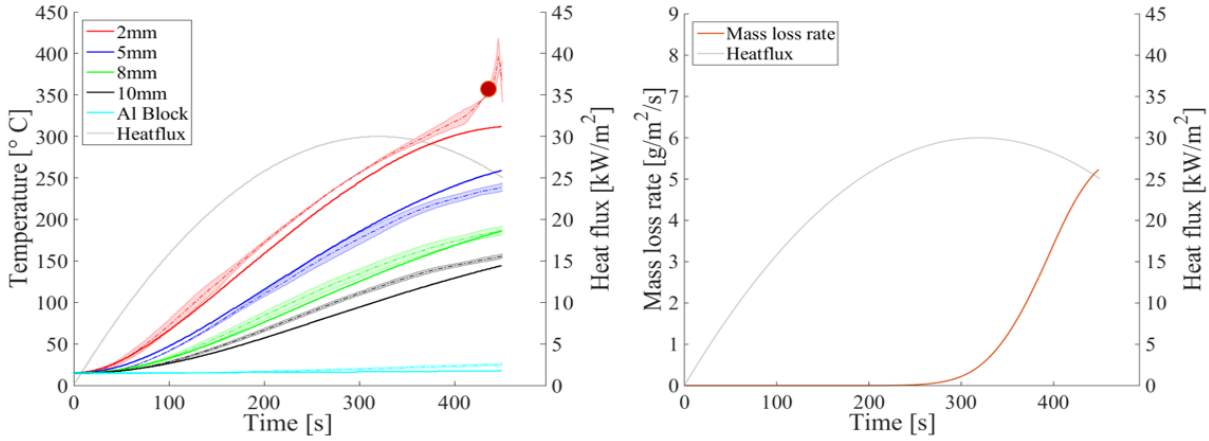

Figure 11: Transient irradiation peaking at 30kW/m^2 after 320s: Temperature(a) and predicted mass loss (b) response at different depths of a PMMA sample; Predictions shown in solid, experiments with dashed line; Error ranges are shown as clouds (sometimes too thin to see); Ignition marked with red dot

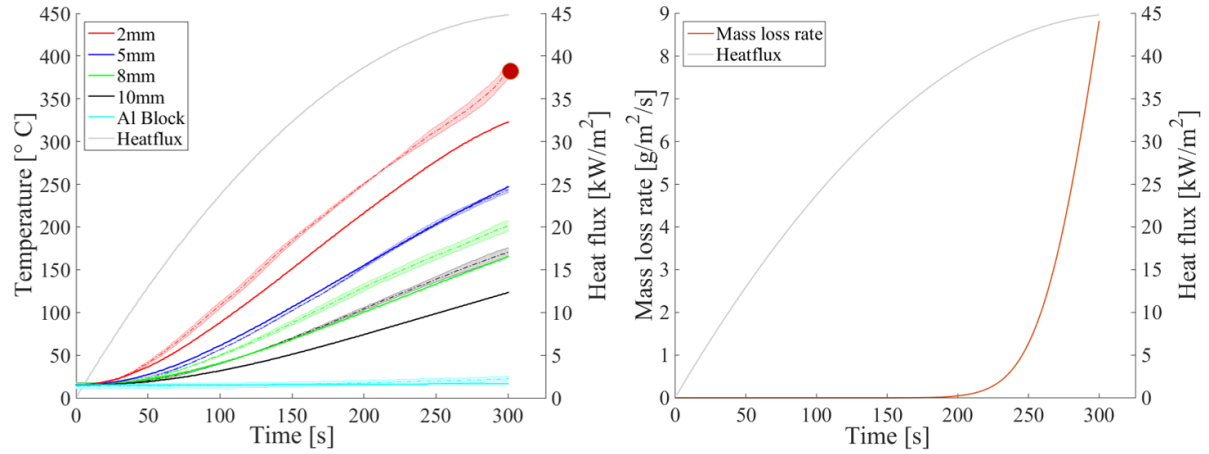

Figure 12: Transient irradiation peaking at 45kW/m^2 after 320s: Temperature(a) and predicted mass loss (b) response at different depths of a PMMA sample; Predictions shown in solid, experiments with dashed line; Error ranges are shown as clouds (sometimes too thin to see); Ignition marked with red dot

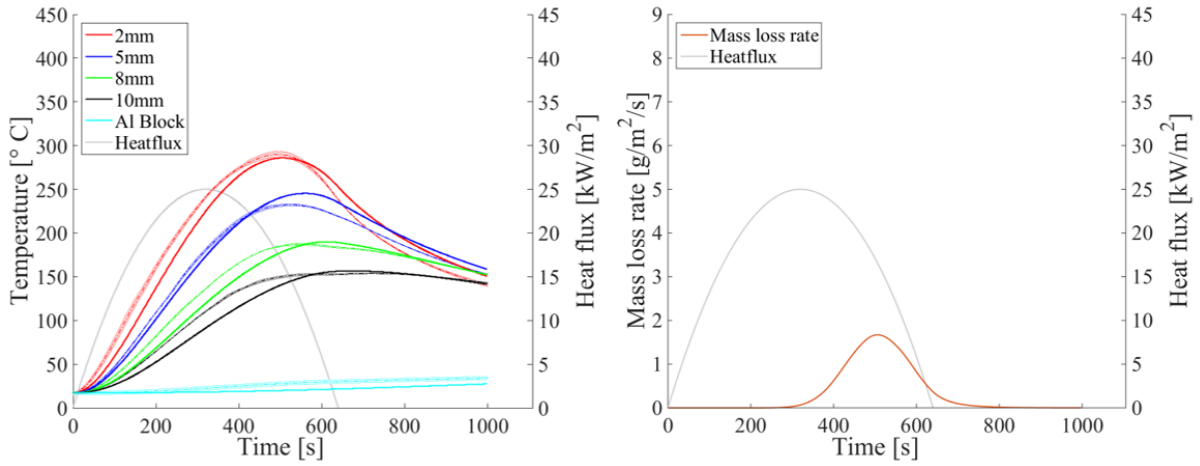

Figure 13: Transient irradiation peaking at 25kW/m^2 after 320s: Temperature(a) and predicted mass loss (b) response at different depths of a PMMA sample; Predictions shown in solid, experiments with dashed line; Error ranges are shown as clouds (sometimes too thin to see)

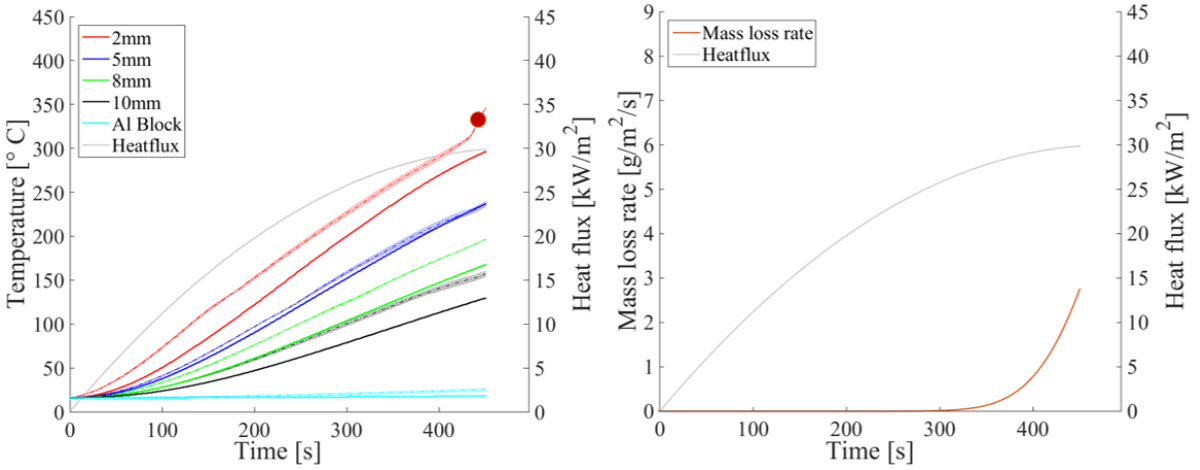

Figure 14: Transient irradiation peaking at 30kW/m^2 after 480s: Temperature(a) and predicted mass loss (b) response at different depths of a PMMA sample; Predictions shown in solid, experiments with dashed line; Error ranges are shown as clouds (sometimes too thin to see); Ignition marked with a red dot

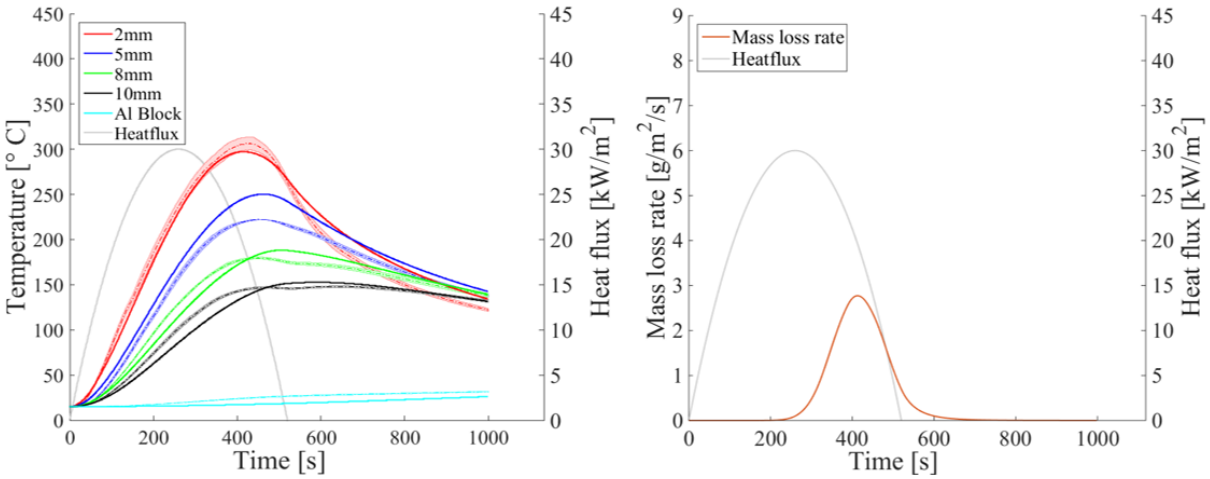

Figure 15: Transient irradiation peaking at 30kW/m^2 after 260s: Temperature(a) and predicted mass loss (b) response at different depths of a PMMA sample; Predictions shown in solid, experiments with dashed line; Error ranges are shown as clouds (sometimes too thin to see)

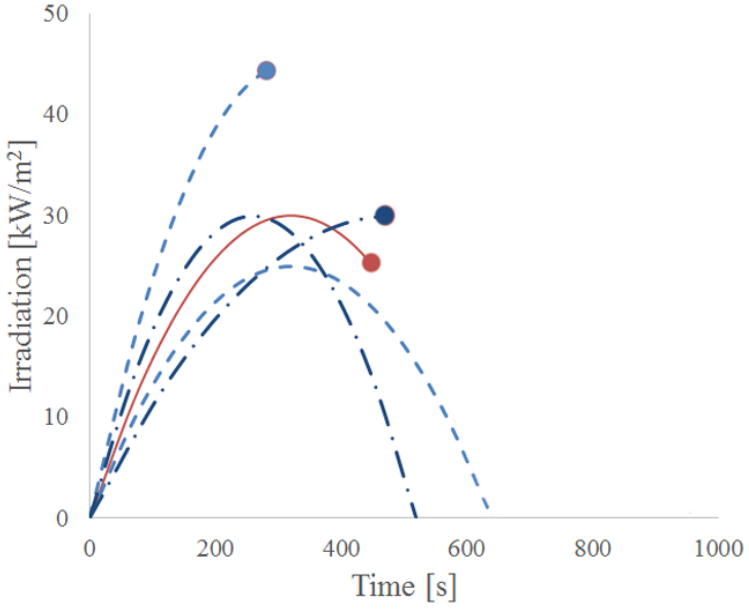

Figure 16: Overview of experimental measurements of the time to ignition for all transient irradiation pulses. The ones where ignition occurred, the irradiation pulse is shown only until ignition time.

5.1. Ignition Criteria

This section analyzes how the different ignition criteria fare in constant and transient irradiation conditions. The four criteria presented previously in Section 2 are implemented such that their validity is investigated using all the experimental and numerical data available in the study. Table 11 summarizes these results and compares them to values from literature.

Table 11: Ignition conditions as observed in experiments and predictions; ignition criteria used, in order: critical temperature, critical energy, time-energy squared, critical mass loss rate (Note*: T_{max} and $\dot{m}''_{max}$ when ignition did not occur; Note**: $Q_{total} = \int_0^{t_{end}} \dot{q}''_e dt$, where t_{end} is the time to the end of experiment where ignition did not occur)

Experiment	t_{ig} (s)	T_{ig} (°C)	T_{max}* (°C)	Q_{ig} (Eq .2) (MJ/m^2)	Q_{total}** (MJ/m^2)	C (Eq. 3) (GJ^2/m^4-s)	$\dot{m}''_{ig}$ (g/m^2-s)	$\dot{m}''_{max}$* (g/m^2-s)
15kW/m^2 constant	-	-	330	-	60	-	-	2.5
20kW/m^2 constant	520	320	-	11.2	-	240	4.9	-
30kW/m^2 at 320s	450	360	-	10.0	-	222	5.2	-
45kW/m^2 at 320s	300	383	-	8.8	-	258	9.0	-
25kW/m^2 at 320s	-	-	290	-	10.7	-	-	1.7
30kW/m^2 at 480s	475	335	-	9.4	-	186	4.1	-
30kW/m^2 at 260s	-	-	306	-	10.4	-	-	2.8
Literature	-	380[4]	-	2 [5]	-	226 [6]	3.0 [11]	-

The critical energy criterion has similar values for all the experiments, regardless whether ignition occurred or not. This lack of resolution makes it impossible to establish a value ignition.

The criterion which uses the time-energy squared correlation proves to have limited applicability. As shown in [6], there is a proportionality factor between the time and the energy-squared. However, this proportionality factor is dependent on the irradiation scenario.

The critical mass loss rate provides a wide range of critical values (from 4.1 to 9g/m^2-s), limiting the accuracy of the the criterion. As shown in Fig. 17, the samples that did not ignite show a mass loss range below the literature value of 3g/m^2-s. Therefore the concept of minimum threshold for mass loss rate is introduced, below which ignition will not occur. However, the mass loss rate results were obtained numerically and need experimental confirmation. Overall, this threshold seems to be the most viable way of estimating whether or not ignition will occur.

The next criterion is the critical temperature. This criterion has shown a capability of estimating a range of temperatures at which PMMA will ignite, with an average of 350°C. The range of critical temperatures is wide (from 320 to 384°C) and the criteria provides a range of times to ignition. Nevertheless, similar to the mass loss rate, our data shows a minimum threshold value, below which ignition does not occur. Fig. 17 collects all the mass

loss rate and temperature information from the experiments and predictions in this work. Observing the trend, the threshold value for temperature is around 305°C.

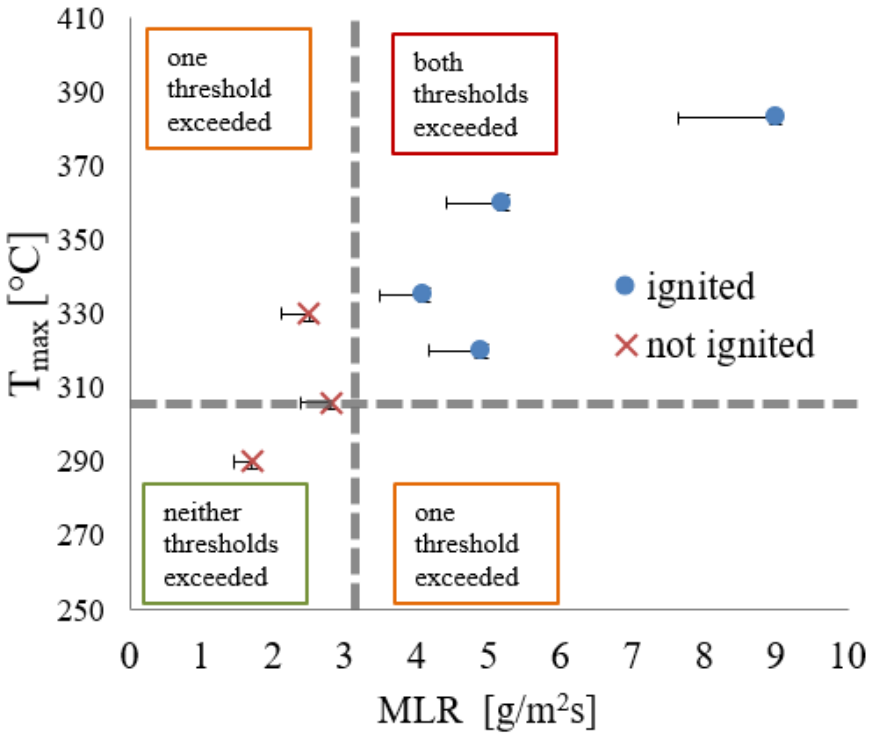

Figure 17: Minimum threshold values for mass loss rate and temperature; the lower left part of the plot shows the area where ignition will not occur (i.e. under a mass loss rate of 3g/m^2-s and a temperature of 305°C) and the upper right part represents the area where ignition will occur

This analysis shows that the minimum thresholds for mass loss rate and temperature offers the earliest possible time to ignition, the other criteria estimate a range of possible ignition times.

6. Predictions using the Minimum Threshold for Mass Loss Rate and Temperature

In the absence of more experiments, the model was used to predict the ignition of 21 more scenarios using the critical mass loss rate criterion. As it was observed in Table 11, when mass loss rate did not reach 3g/m^2-s, the sample did not ignite. Therefore, this value was taken as a reference for establishing whether or not ignition occurs.

Table 12 also shows the good correlation between the minimum threshold for mass loss rate and the minimum threshold for temperature. The values of temperature when the sample

reaches a mass loss rate of 3g/m^2-s fall mostly in the range of 300-305°C. Based on the ignition experimental results presented in Table 11 as well as the modeling application, a value of 305°C is chosen as a threshold. In the case when a sample passes both minimum thresholds, ignition is guaranteed to take place, whereas if neither thresholds are reached, ignition will not occur. This provides a conservative approach to establish the earliest possible time to ignition.

The scenarios used in this application have peak irradiation ranging from 15kW/m^2 to 100kW/m^2. The times to peak irradiation are 160s, 320s and 480s. A summary of the scenarios and their time to ignition, if it occurs, is shown in Table 12.

Table 12: Ignition predictions using the model and a critical mass loss value of 3g/m^2-s

Scenario	**Peak Irradiation** (kW/m^2)	**Time to Peak** (s)	**Time to Ignition** (s)	**Temperature at Ignition** (°C)
1	15	160	-	-
2	15	320	-	-
3	15	480	-	-
4	20	160	-	-
5	20	320	-	-
6	20	480	-	
7	35	160	-	-
8	35	320	331	300
9	35	480	395	300
10	40	160	-	-
11	40	320	294	301
12	40	480	355	300
13	50	160	186	305
14	50	320	245	303
15	50	480	300	302
16	70	160	307	
17	70	320	193	306
18	70	480	238	304
19	100	160	110	313
20	100	320	189	361
21	100	480	190	308

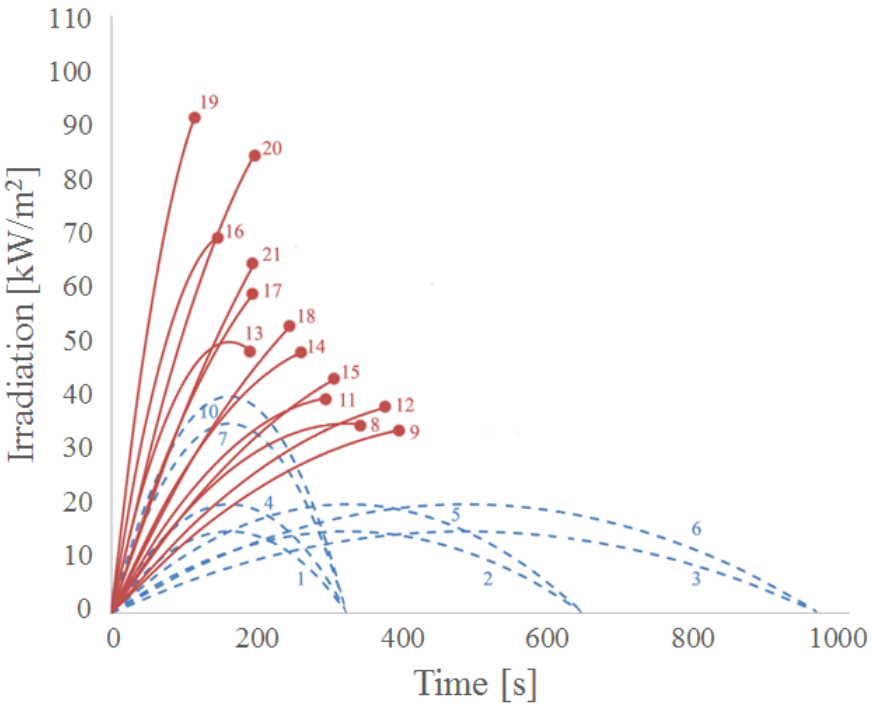

Figure 18: Predicted time to ignition of different parabolic heat fluxes using a critical mass loss rate of 3g/m^2-s

Fig. 18 summarises the results of the simulations presented in Table 12. When exposed to a low irradiation of 15 or 20kW/m^2, the sample is predicted to not ignite, regardless of the heating rate, because the mass loss rate never reaches 3g/m^2-s. The same is valid when 35 or 40kW/m^2 is reached at 160s, when the sample does not ignite because the exposure to the irradiation is not long enough. In all the other scenarios, the model predicts that the sample will ignite. The results of the predicted times to ignition show that the at high heat fluxes (over 50kW/m^2), the samples will ignite faster when the time to peak is shorter. When the irradiation is lower, such a short time to peak does not produce a high enough mass loss rate to cause ignition.

7. Conclusion

We have used transient irradiation to study the process of pyrolysis and ignition of PMMA samples by combining computational and experimental approaches.

Heating a fuel sample with transient irradiation is a much more realistic fire scenario than a constant source. Moreover, transient irradiation is the comprehensive scenario for fire research and the general case for solid ignition. Apart from the present work, all but two studies in the fire science literature consider constant irradiation.

We have investigated transient irradiation with parabolic pulses (simplest curve including both growth and decay) which for the base case is at 30kW/m^2 after 320s. The base case is then altered to investigate the influence of increasing and decreasing the peak heat flux (45 and 25kW/m^2) and the time to peak (480 and 320s). The model, based on heat transfer, single step chemistry and temperature dependent properties, was validated first against benchmark experimental data [9] under constant irradiation. The comparison with the transient irradiation shows good agreements with the measured in-depth temperature profiles with an average error below 9%.

Model and experiments are combined to study the validity of the different ignition criteria found in the literature. We find that of these criteria, the best predictions are provided by the critical mass loss rate followed by the critical temperature, and the worst is the critical energy.

Further analysis reveals the novel concept of simultaneous minimum threshold values. While the mass loss rate is below 3g/m^2 and the surface temperature is below 305°C, ignition does not occur. Therefore these threshold values when exceeded simultaneously establish the earliest time possible for ignition.

Acknowledgements

The authors thank FM Global for funding this work. Also, the support of Juan Hidalgo-Medina in assisting with the experimental set-up and the input of Xinyan Huang are gratefully acknowledged.

Bibliography

[1] H. Hottel, Combustion Science and Technology 39 (1984) 1–10.
[2] A. Fernandez-Pello, in: Fire Safety Science - Proceedings of the Tenth International Symposium, Internatonal Association for Fire Safety Science, pp. 25–42.
[3] D. Drysdale, in: An Introduction to Fire Dynamics, John Wiley and Sons, 2011, pp. pp. 225–275.
[4] J. Torero, in: SFPE Handbook of Fire Protection Engineering, National Fire Protection Association, 4th edition, 2008, pp. pp. 2–260–2–277.
[5] V. Babrauskas, in: Ignition Handbook, Fire Science Publishers, 2003, pp. pp. 234–251.
[6] P. Reszka, P. Borowiec, T. Steinhaus, J. Torero, Combustion and Flame 159 (2012) 3652–3657.
[7] C. Belcher, R. Hadden, G. Rein, J. Morgan, N. Artemieva, T. Goldin, Journal of the Geological Society (2015).
[8] C. Lautenberger, C. Fernandez-Pello, Fire Safety Journal 44 (2009) 819–839.
[9] T. Kashiwagi, T. J. Ohlemiller, Symposium (International) on Combustion 19 (1982) 815–823.
[10] N. Bal, G. Rein, Combustion and Flame 158 (2011) 1109–1116.
[11] D. Rich, C. Lautenberger, J. L. Torero, J. Quintiere, C. Fernandez-Pello, Proceedings of the Combustion Institute 31 (2007) 2653–2660.
[12] D. Spalding, Some fundamentals of combustion, Butterworths, London, 1955.
[13] H. Thomson, D. Drysdale, Fire Safety Science 2 (1988) 67–76.
[14] R. Lyon, J. Quintiere, Combustion and Flame 151 (2007) 551–559.

[15] N. Bal, Uncertainty and complexity in pyrolysis modelling, Ph.D. thesis, The University of Edinburgh, 2012.
[16] ASTM Standard E2058, Standard Test Methods for Measurement of Material Flammability Using a Fire Propagation Apparatus (FPA), Technical Report, West Conshohocken,PA, 2013.
[17] P. Reszka, J. Torero, Experimental Thermal and Fluid Science 32 (2008) 1405–1411.
[18] R. Carvel, T. Steinhaus, G. Rein, J. Torero, Polymer Degradation and Stability 96 (2011) 314–319.
[19] C. W. Lautenberger, Gpyro A Generalized Pyrolysis Model for Combustible Solids Technical Reference, Technical Report, Department of Mechanical Engineering University of California , Berkeley, Berkeley, 2009.
[20] N. Bal, G. Rein, Fire Safety Journal 61 (2013) 36–44.
[21] C. W. Lautenberger, A generalized pyrolysis model for combustible solids, Ph.D. thesis, University of California, Berkeley, 2007.
[22] European Aluminium Association, Aluminium: Physical properties, characterisitics and alloys. Technical Report, Technical Report, Banbury, UK, 1994.
[23] N. Bal, J. Raynard, G. Rein, J. Torero, M. Försth, P. Boulet, G. Parent, Z. Acem, G. Linteris, International Journal of Heat and Mass Transfer 61 (2013) 742–748.